

# Design of a Compact Ka-band Monopulse Cassegrain Antenna

Tenigeer <sup>(1)</sup>, Wilson Tang <sup>(1)</sup>, Dhanraj Doshi <sup>(1)</sup>, and Yonghui Shu <sup>(1)</sup>  
 (1) Eravant, Torrance, CA 90501, USA (fn-tenigeer@eravant.com)

**Abstract**— This paper presents a 24-inch aperture monopulse reflector antenna. A novel design approach for the sum-and-difference network is integrated using folded Magic-Ts to achieve a compact structural design. Furthermore, the feed network utilizes a Cassegrain configuration while the feed system employs a dielectric-rod-loaded four-horn feed to condense the package size. A prototype was fabricated and tested, with the experimental results showing good agreement with the simulations. The antenna exhibits excellent performance across the 34–36 GHz band with about 35 dBi overall null depth, validating the effectiveness and accuracy of the proposed compact design. This further demonstrates soundness of the manufacturing process and measurement accuracy.

## I. INTRODUCTION

With the rapid advancement of technologies such as missiles, rockets, satellites, and aerospace, the requirements for antenna tracking accuracy have become increasingly stringent. Common automatic tracking methods for reflector antennas include step tracking, conical scan tracking, and monopulse tracking. Among these, monopulse tracking offers the highest precision and superior performance. Monopulse tracking antennas can automatically guide, search, and track high-speed flight vehicles. Due to their excellent tracking capabilities, they are widely utilized in various fields such as satellite communications, remote sensing and telemetry, and radar systems [1] [2]. Tracking for these applications is guided by a null point that indicates the position of the target.

The operating principle of a monopulse antenna is that when the antenna is aligned with the target, the null point of the difference beam points exactly at the target. At this moment, the energy received by each horn is equal, and no error signal is generated. If the target moves off-axis—meaning it deviates from the null point of the difference beam—the energy within each horn becomes unbalanced. The sensitive components then generate an error signal. The radar detects the target's displacement by comparing the amplitudes of the echo signals excited in each horn. To achieve this detection effect, the monopulse antenna employs a feed network comprised of multiple feed horns.

Monopulse feeds come in various forms, with four-horn and five-horn configurations being the most commonly used. In a four-horn feed, the sum and difference beams share the same aperture; while this results in a compact structure, it leads to a significant sum-difference conflict. Conversely, a five-horn feed employs independent apertures for the sum and difference beams. This increases the physical size, which can easily cause blockage in reflector antennas with medium gain, leading to

higher side-lobe levels. However, the five-horn feed offers the advantage of a lower sum-difference conflict. While considering these design aspects, integrated dielectric loading can aid in reducing the package size of the feed network and offset the issues of typical four-horn configurations to produce a significantly compact feed network design.

## II. MONOPULSE FEED NETWORK DESIGN

To counteract the drawbacks of a four-horn configuration, dielectric loading was attached to the four A, B, C, and D feed quadrants shown in Fig. 1 illustrating a typical comparator network. By using dielectric loading, the gain can be increased without enlarging the feed aperture [3] [4], while simultaneously ensuring that the sum beam of the feed maintains a low side-lobe level. To further reduce side lobes, a choke structure is added to the outermost periphery of the four horns. Additional improvements to the design were implemented to further reduce the size of the feed network.

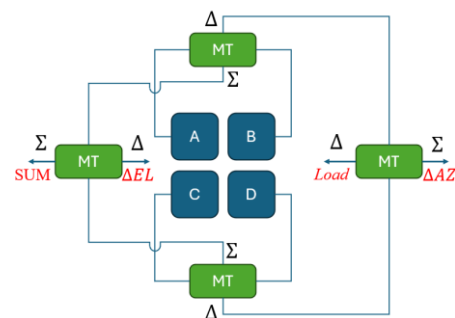


Figure 1. Block Diagram of Comparator Network.

To make the feed network more compact, the sum-difference network adopts a Folded Magic Tee (FMT) configuration. First, the four horns are connected to two H-plane FMTs; their sum ports are then connected to an E-plane FMT to form the sum beam port and the elevation difference beam port. The difference ports of the two H-plane FMTs are connected to a standard Magic Tee (MT), ultimately forming the azimuth difference port. The specific relationships are as follows with Fig. 1 as reference:

$$SUM = A + B + C + D \quad (1)$$

$$\Delta EL = (A + B) - (C + D) \quad (2)$$

$$\Delta AZ = (A + C) - (B + D) \quad (3)$$

$$LOAD = (A - B) - (C - D) \quad (4)$$

With the basic framework of the design established, the general feed network was conceived as shown in Fig. 2, which features the dielectric loading rods. The rods are made of high-density polyethylene (HDPE). Inside the waveguides, a stepped structure is employed for impedance matching to minimize the VSWR (Voltage Standing Wave Ratio). The entire assembly adopts a symmetrical design, ensuring identical electrical path lengths from any input port to the four radiating horns. By simplifying the magic tee structure along with using dielectric loading rods, the network was compressed to a package size of approximately 6.2" (L) x 3.6" (W) x 2.1" (H) or 2.6" (L) long without the horns. With the general structure of the comparator completed, a system of reflectors was deployed to complete the monopulse Cassegrain antenna design.

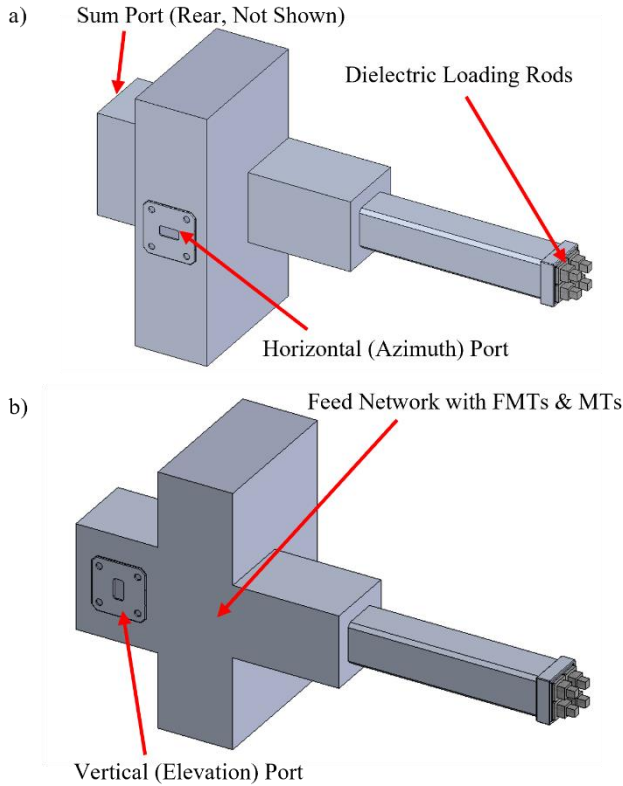


Figure 2. Simplified Comparator Network Structure. (a) Isometric View Highlighting Horizontal (Azimuth) Port. (b) Isometric View Highlighting Vertical (Elevation) Port.

### III. REFLECTOR DESIGN

Due to the large physical size of the monopulse feed network, using a single-reflector antenna would result in significant blockage, thereby reducing the overall antenna efficiency. To address this, a dual-reflector configuration is adopted to position the feed behind the main reflector, effectively alleviating the feed blockage issue. A common type of dual-reflector antenna is the Cassegrain antenna. It consists of a paraboloid as the main reflector and a hyperboloid as the sub-reflector. One focus of the hyperboloid coincides with the focal point of the paraboloid, while the feed is placed at the other focus of the hyperboloid [5]. To facilitate the dual-reflector design process, the geometrical relationships between the feed aperture and reflectors were established.

As shown in Fig. 3, the Cassegrain antenna is defined by seven primary parameters:  $D_m$  is the aperture diameter of the paraboloid;  $F_m$  is the focal length of the paraboloid;  $\alpha$  is the half-aperture angle of the main reflector, which also represents the half-illumination angle from the virtual feed to the antenna;  $D_s$  is the diameter of the hyperboloid, i.e., the sub-reflector diameter;  $\theta$  is the half-illumination angle of the feed toward the sub-reflector; and  $2c$  is the distance between the virtual focus  $F_2$  and the real focus  $F_1$ , representing the focal length of the hyperbola.

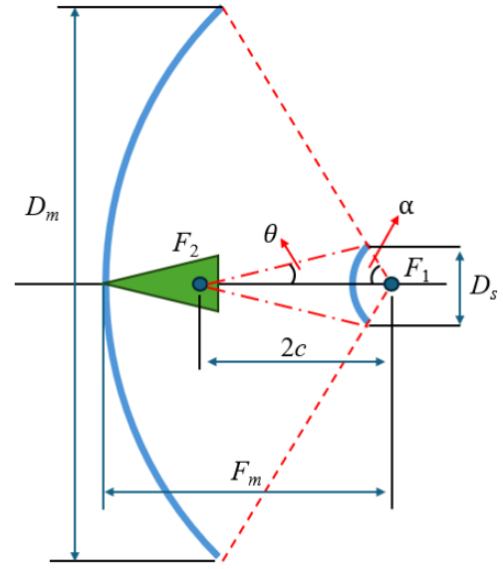


Figure 3. Geometric Relationships of the Cassegrain Antenna.

Among these,  $D_m$ ,  $F_m$ ,  $D_s$ , and  $\theta$  are designated as independent parameters, which must be determined based on specific requirements to derive all other geometric parameters of the Cassegrain antenna. The selection principles for these independent parameters are as follows:

1) *Determining the aperture diameter:*  $D_m$  is determined based on the gain requirements, and its value can be derived using the antenna gain formula:

$$G = \frac{4\pi S}{\lambda^2} \eta \quad (2)$$

Where  $S$  represents the aperture area of the paraboloid and  $\eta$  is the aperture efficiency. For dual-reflector antennas,  $\eta$  is typically chosen between 50% and 60%.

2) *Determining the focal length:*  $F_m$  is determined by the focal-length-to-diameter ratio. For long focal length designs,  $F_m / D_m$  typically ranges from 0.3 to 0.5. A larger  $F_m / D_m$  can enhance the performance of the feed during off-axis operation, resulting in a shallower parabolic depth and lower cross-polarization. Conversely, a smaller  $F_m / D_m$  reduces the minimum blockage ratio and shortens the forward protrusion of the feed.

3) *Determining the sub-reflector diameter:* A smaller  $D_s$  helps to reduce the side-lobe levels (SLL). However, if  $D_s$  is too

small, the physical size of the feed may exceed the sub-reflector's diameter, leading to an increased blockage ratio. Conversely, an excessively large  $D_s$  will also intensify the blockage effect. Therefore, in engineering practice, the ratio  $D_s / D_m$  is typically chosen between 0.1 and 0.2.

4) *Selection for  $\theta$* : For Cassegrain antennas with gain requirements below 50 dB, a feed with a gain of 15–18 dB is typically selected, corresponding to a 10 dB beam half-angle of 25°–30°.

Ultimately, the antenna parameters designed in this paper are summarized in Table I. Using these parameters, the design envelope and geometry was established to complete the mechanical design of the monopulse antenna. Various assembly approaches and design considerations were employed to further reduce the package size and complexity in order to fabricate the completed antenna design.

TABLE I. SUMMARY OF ANTENNA PARAMETERS.

$D_m$	$F_m / D_m$	$D_s$	$\theta$
24	0.192	3.36	28

#### IV. FABRICATION AND MEASUREMENT

The fabricated prototype of the antenna is shown in Fig. 4. The feed assembly is machined from aluminum, while the dielectric rods are made of HDPE with a relative permittivity of  $\epsilon_r = 2.35$ . The antenna features three ports: the sum channel, the

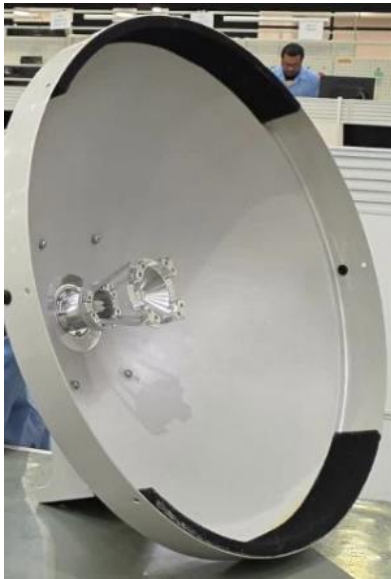


Figure 4. Fabricated Prototype of Monopulse Antenna.

horizontal (azimuth) difference channel, and the vertical (elevation) difference channel as described in Fig. 2. Fig. 5 illustrates the return loss for these three ports. As observed, the return loss for all ports remains below -15 dB across the operating band. Simultaneously, the isolation between the sum and difference ports was also measured as shown in Fig. 6. As shown in the figure below, the isolation levels between the sum port and the difference ports are all below -30 dB.

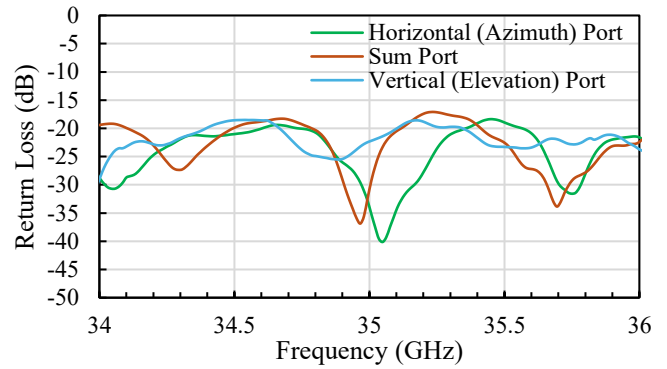


Figure 5. Return Loss of Sum, Azimuth, and Elevation Ports.

The radiation characteristics of the antenna are shown in Fig. 7 to 10, including the sum and difference beam patterns. It can be observed that the null depth of the difference beams reaches below -30 dB. The final measured results indicate that the antenna achieves a sum-channel gain of 42 dB and a difference-channel gain of 35 dB. The 3 dB beamwidth of the sum beam is 2°, and the side-lobe levels (SLL) are consistently below -15 dB. Measured radiation results show good agreement with simulated patterns and excellent performance as summarized in Table II.

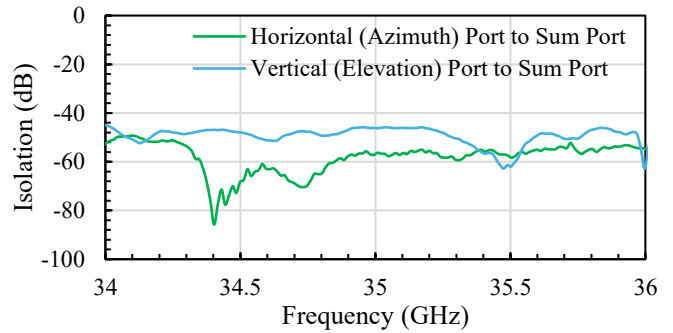


Figure 6. Isolation Between Sum and Difference Ports

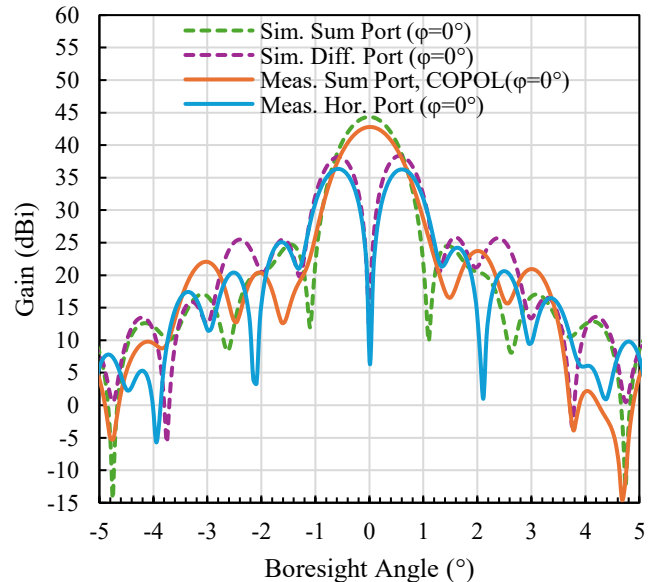


Figure 7. Simulated vs. Measured Radiation Characteristics at 35 GHz for Sum and Horizontal Ports

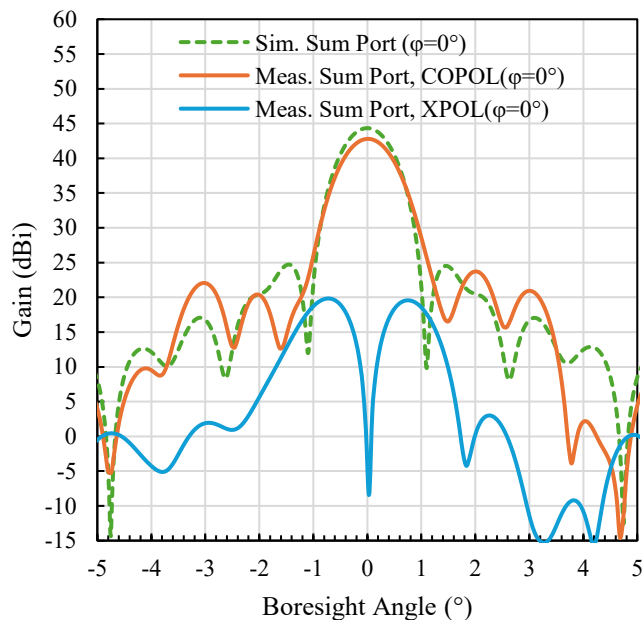


Figure 8. Simulated vs. Measured Radiation Characteristics at 35 GHz for Sum Port Copolarization and Cross-polarization.

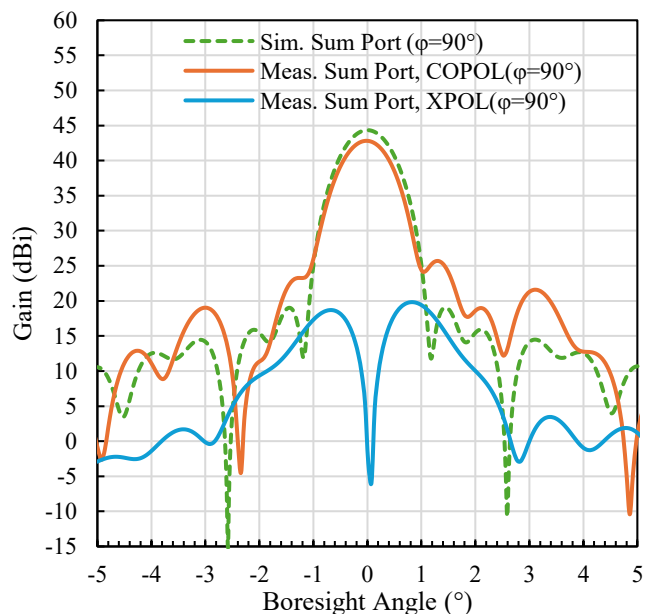


Figure 10. Simulated vs. Measured Radiation Characteristics at 35 GHz for Sum Port Copolarization and Cross-polarization.

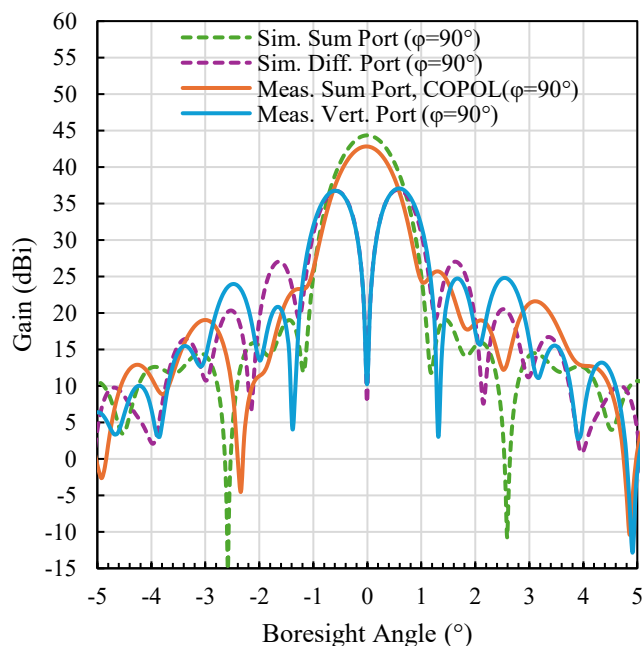


Figure 9. Simulated vs. Measured Radiation Characteristics at 35 GHz for Sum and Vertical Ports.

TABLE II. SUMMARY OF ANTENNA PERFORMANCE PARAMETERS.

Frequency	34 GHz	35 GHz	36 GHz
Gain, Sum (dBi)	42.79	43.08	42.77
Gain, Difference (V) (dBi)	36.97	37.53	37.60
Gain, Difference (H) (dBi)	36.00	36.23	36.16
Null Depth, (V) (dBi)	35.71	32.61	34.33
Null Depth, (H) (dBi)	34.00	36.51	38.61
3 dB BW (°)	0.93	0.92	0.87

## V. CONCLUSION

This paper presents a compact monopulse Cassegrain antenna. By utilizing dielectric rod loading and a folded Magic-T, the feed network is made more compact while achieving excellent measured return loss of below -15 dB across the operating range along with gain for the sum port of approximately 43 dBi and difference port of approximately 37 dBi. The measured results are in good agreement with the simulated ones, demonstrating significant practical application value.

## ACKNOWLEDGMENT

The authors would like to thank Eravant's passive line team for assembling the monopulse antenna for pattern testing. The authors would also like to thank Alexander Chen, Craig Roberts, and Dayong Yang from the Eravant on setting up the inhouse near-field range, without which, we wouldn't be able to capture the radiation patterns of the compact monopulse Cassegrain antenna discussed in the paper.

## REFERENCES

- [1] Zhao, Jianing, et al. "A compact Ka-band monopulse Cassegrain antenna based on reflectarray elements." *IEEE Antennas and Wireless Propagation Letters* 17.2 (2017): 193-196.
- [2] Chen, Zhi Xing, et al. "Design of a Wideband High-Gain Monopulse Antenna for X-and Ku-Bands Applications." *IEEE Access* (2024).
- [3] Qian, Song-song, Xing-guo Li, and Ben-qing Wang. "Ka band Cassegrain monopulse antenna fed by tapered rod antennas." *2008 8th International Symposium on Antennas, Propagation and EM Theory*. IEEE, 2008.
- [4] Kumar, Chandrakanta, V. Senthil Kumar, and V. V. Srinivasan. "Design aspects of a compact dual band feed using dielectric rod antennas with multiple element monopulse tracking." *IEEE Transactions on Antennas and Propagation* 61.10 (2013): 4926-4932.
- [5] Zheng, Pei, et al. "Design of a W-band full-polarization monopulse Cassegrain antenna." *IEEE Antennas and Wireless Propagation Letters* 16 (2016): 99-103.